

ANALYSIS OF STRAIN IN FINGER-JOINTED LUMBER

Roland Hernandez

Finger jointing is used in various structural, sub-structural, and nonstructural applications. This paper discusses preliminary experimental evaluation of the structural finger-joint profile commonly used in U.S. glued-laminated timber (glulam) manufacture today. Moiré interferometry was used to obtain full-held fringe patterns of finger-joint specimen in tension. From the moiré fringe patterns, longitudinal, transverse, and shear strains were calculated at various locations in the finger joint profile. From these calculated strains, various elastic properties of the adherends as well as regions of high strain ratios were determined.

1. INTRODUCTION

End jointing of lumber to permit the use of single-piece construction has been used extensively since the early 1900s, when it was used for aircraft construction. This end-jointing technique used a sloped scarf as a means of bonding two pieces of lumber end-to-end. The scarf-joint design was developed because end-grain bonding of wood has little structural capacity. Therefore, the scarf joints were machined so that the adhesive bond was nearly parallel to the grain of the wood.

Beginning in about the 1950s, several researchers studied variations of end-joint profiles in efforts to produce a joint with adequate structural capacity while not increasing the volume of wood that had to be machined. This resulted in development of the modern-day finger joint, which was based on the parameters shown in figure 1.

These parameters are pitch (P), finger length (L), tip thickness (t), and slope ($\tan \theta$). This design was based on maintaining the slope of the fingers equal to that of the scarf-joint design, except that the overall length of the joint was greatly reduced. The parameters for the most common structural finger-joint profiles used in the manufacture of U.S. glulam today are shown in table 2.

For a given cross-sectional dimension of lumber, the bonded surface area of this finger-joint geometry is nearly equal to that of a scarf joint that has the same slope. However, the finger-joint profile only requires about 10 percent of the volume of wood to be removed compared with that of a scarf joint.

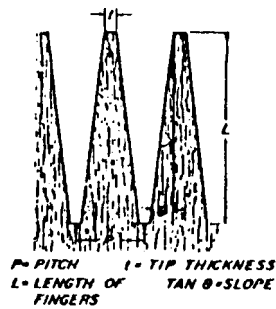


Fig. 1 Typical finger joint with geometric parameters identified.

Parameter	Profile 1	Profile 2
Length	28.27 mm (1.113 in.)	28.27 mm (1.113 in.)
Pitch	6.985 mm (0.275 in.)	6.731 mm (0.265 in.)
Tip thickness	0.813 mm (0.032 in.)	0.762 mm (0.030 in.)
Slope	1:10.55	1:10.86

Table 2 Geometric parameters of structural finger-joint profiles used in U.S. glulam manufacture.

2. OBJECTIVES

The primary objective of this study is to present preliminary results of advanced experimental evaluation of the common structural finger-joint profile used in U.S. glulam manufacture today. Moiré interferometry was used because this method possesses a high resolution for measuring strains around the finger profile. In addition, full-fold strain behavior can be observed with this experimental method.

3. BACKGROUND

3.1 Development of finger-jointed lumber designs

Historically, the performance of end-jointed lumber has been evaluated by comparing its tensile strength performance to that of solid-sawm lumber, commonly referred to as joint efficiency. Joint efficiencies in the range of 80 to 100 percent have been reported in various studies [1] and unpublished research for scarf joints that have slopes in the range of 1:10 to 1:20. In the early 1950s, several different types of end-jointing methods were studied for possible replacement of the scarf joint in glulam manufacture [1]. In other independently conducted studies [2-10] and unpublished research, the effects of the geometric parameters shown in figure 1 on finger-joint tensile strength were studied. In general, all of these studies found that as the slope of the fingers decreased, the tensile strength of the finger joints increased. However, the rate of increase in tensile strength diminished for slopes of 1:12 and flatter. All these studies also reported that the geometric parameter that most significantly influenced finger-joint strength was the tip thickness. That is, the smaller the tip thickness dimension, the stronger the finger joint.

With the established fact that tip thickness was the limiting factor in finger-joint strength, other studies were conducted that targeted finger-joint designs that produced near feather-tipped fingers [11-13].

3.2 Analytical evaluation of finger-jointed lumber

All of the studies discussed up to now focused on using experimental strength results of various finger-joint designs relative to solid-sawn lumber. A wide range of geometric parameters were studied to enable the researchers to design a finger joint with optimal balance between strength, material waste, and cutter durability. Although the effect of the geometric parameters from figure 1 were well understood, analytical methods had not been applied to finger-joint design.

Beginning in the 1980s, the use of the finite element method as a research tool was becoming commonplace in the wood industry. Several studies involving analysis of finger-jointed lumber appeared in the literature [14-18]. In general, the researchers reached conclusions similar to those of the experimental studies from previous years. That is, that decreasing tip thickness resulted in increased finger-joint strength. More refined statements were made regarding the geometric parameters from figure 1. For example, strength gains were minimal beyond a length of 30 mm (1.181 in.) and tip thickness should not exceed 0.5 to 0.7 mm (0.020-0.028 in.) [16]. Other findings of these analytical studies were that finger-joint stresses were reduced when glue-line plasticity was increased [14-16] and that stresses increased as the ratio of material properties from both sides of the joint increased [15].

3.3 Evaluation of strain distributions in bonded joints

Pellicane et al. [17] were the first researchers to experimentally measure the strain distributions in a finger joint, in that study, an optical photographic method and microstrain gages were used. Both methods provided strain measurements, however, the photographic method was only applicable across a gage length of 38 mm (1.42 in.), and the microstrain gages were 1.27 mm (0.05 in.) long. Although the sensitivity of the microstrain gages is adequate for evacuating strains around finger joints, this experimental method is dependent on the location of the gages and was greatly influenced by localized deviations such as earlywood and latewood bands as well as localized slope of grain.

Recently, Zink et al. [18] applied a computer vision white light speckle technique to measure the strain distribution in a double-lap wood joint. Full-field strain distributions obtained with this method showed that both transverse and shear strains existed along the glue-lines and that these strains significantly increased at the end of the overlaps. The gage length used in this study for measuring transverse strains was 0.5 mm (0.02 in.).

4. RESEARCH METHODS

This study examines the use of moiré interferometry for characterizing strain distributions in finger-jointed lumber. Full-field moiré fringe patterns were obtained and analyzed for longitudinal, transverse, and shear strain at various locations throughout the profile.

4.1 Moiré Interferometry

Although moiré interferometry is not new, there has been little research in applying this experimental technique to wood. Some examples of past moiré research dealing with wood include studies of strains due to hygroscopic movement, lumber drying, and bolted connections [19-21].

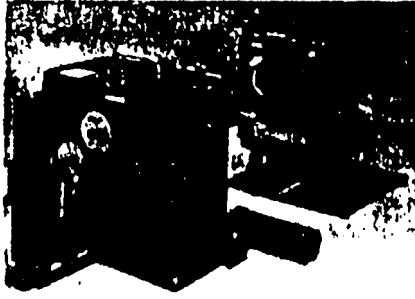


Fig. 3 Compact moiré interferometer (foreground) and Polaroid camera (background).

The test apparatus used in this study was a compact moiré interferometer (fig. 3) with a grid resolution of 2400 lines per millimeter (60,960 lines per inch). The theoretical gage length for moiré interferometry with a grid resolution of 2400 lines per millimeter is $0.42 \mu\text{m}$ ($1.64 \times 10^{-5} \text{in.}$). This resolution corresponds to measurable strain at approximately 0.20 MPa (29 lb/in^2). More details on the techniques used to prepare specimens and conduct the tests are given in Post et al. [22].

The finger-jointed specimens were tested in tension using load-controlled settings of an MTS test machine. The V-field and U-field images were photographed at various levels of load throughout the test. The photographic images were processed into digital images for analysis. The strains in the specimen were calculated from the moiré patterns using the following equations:

$$\epsilon_y = \frac{\partial V}{\partial y} = \frac{1}{f} \left[\frac{\partial N_y}{\partial y} \right] \quad (1)$$

$$\epsilon_x = \frac{\partial U}{\partial x} = \frac{1}{f} \left[\frac{\partial N_x}{\partial x} \right] \quad (2)$$

$$\gamma_{xy} = \frac{\partial U}{\partial y} + \frac{\partial V}{\partial x} = \frac{1}{f} \left[\frac{\partial N_x}{\partial y} + \frac{\partial N_y}{\partial x} \right] \quad (3)$$

where U and V are the fields corresponding to the x and y axes, respectively, ϵ_x and ϵ_y are strains along the x and y axes, respectively, γ_{xy} is shear strain in the x - y plane, f is the frequency of the reference grating (2400 lines per mm), and $\partial N_x / \partial x$, $\partial N_y / \partial y$, $\partial N_x / \partial y$, and $\partial N_y / \partial x$ are the fringe gradients.

6. RESEARCH RESULTS

The specimen presented in this study is shown in figure 4a along with sections where analyses were conducted. The cross-sectional dimensions were 6.0 mm (0.2375 in.) thick by 16.8 mm (0.6595 in.) wide. For this particular specimen, the finger profile is on the L-R plane of the wood adherends. The slope of grain with re-

spect to the global x axis was 88.1° and 93.0° for the top and bottom adherends, respectively.

5.1 Moiré interferometry results

The moiré patterns obtained at a tensile load of 1223 N (274.9 lb) are shown in figure 4b and 4c for the V-field and U-field, respectively. This load was approximately 33 percent of the ultimate failure load in tension.



Fig. 4 (a) finger-joint specimen, (b) V-field and (c) U-field moiré pattern at 1223 N.

For a homogeneous isotropic specimen loaded in tension, one would expect perfectly horizontal moiré fringes in the V-field and perfectly vertical moiré fringes in the U-field. This would correspond to uniform elongation in the direction of the tensile loads and uniform contraction in the transverse direction, also referred to as the Poisson's effect. From figure 4b and 4c, it is apparent that a finger-jointed piece of wood does not exhibit uniform strain in either the longitudinal (V-field) or transverse (U-field) directions.

Figure 4b shows that the near-horizontal fringes in the lower adherend (away from the joint) were closer-spaced than those in the upper adherend. Equation (1) shows that this corresponds to higher strain in the lower adherend, which would result in a lower calculated longitudinal modulus of elasticity (E_L). In the center region near the gluelines, a significant amount of fringe distortion was observed. The region along the fringes that had a positive or negative slope corresponds to increased shear strain due to the loads being transferred across the gluelines. The slope of these distorted fringes tended to be zero at the centerlines of each finger, corresponding to zero shear strain.

In figure 4c, the slopes of the U-field fringes changed from negative slope in the upper adherend to positive slope in the lower adherend. This is due to the slight difference in slope-of-grain angle of the top and bottom adherends. The transition from positive to negative slope occurred near the top of the finger-joint profile, nearer to the higher stiffness adherend. If the E properties of the top and bottom adherends were identical, this transition zone would have occurred at the center of the finger-joint profile. Increased fringe distortion was also observed in the earlywood-late-

wood interfaces. With the use of Equation (2), a comparison of figure 4a and 4c shows that higher transverse strain occurred in the latewood bands of the specimen.

Longitudinal strains (ϵ_{yy}) were calculated using Equation (1) for V-field fringe patterns at tensile loads of 693 and 1223 N. These calculated strains are shown in figure 5a and 5b for Sections A-A and B-B, respectively.

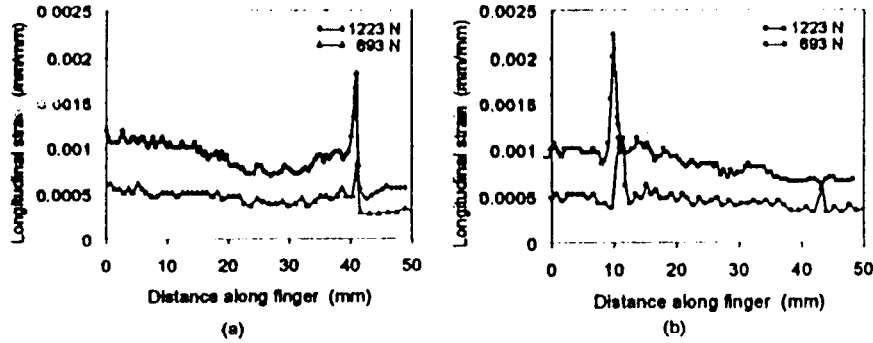


Fig. 5. Longitudinal strains calculated along (a) Sections A-A and (b) Section B-B from figure 4a.

Based on measured strains from two loads (fig. 5a and 5b), the E_L of the adherends was calculated. In Section A-A away from the finger-joint tip, an E_L of 9.59 GPa (1.391×10^5 lb/in²) was calculated for the bottom adherend. From Section B-B, an E_L of 18.2 GPa (2.646×10^5 lb/in²) was calculated for the top adherend. The ratio between the far-field strain and the finger-joint tip strain of Section A-A was 3.39 and 1.69 for tensile loads of 693 and 1223 N, respectively. For Section B-B, the strain ratios were 2.99 and 1.55, respectively. Apparently, the strain ratio effect is a function of load and not a constant value. In addition, Poisson's ratios for each adherend were calculated using the change in transverse strain (ϵ_{xx}) and in ϵ_{yy} . These ratios were 0.33 and 0.23 for top and bottom adherends, respectively.

Section C-C (fig. 4a) shear strains were calculated with Equation (3) using both the V-field and U-field fringe patterns. Figure 6 shows that the maximum shear strain across the center of a finger-joint profile occurs at the glueline and that local deviation in shear strain is also detectable at the earlywood-latewood interface.

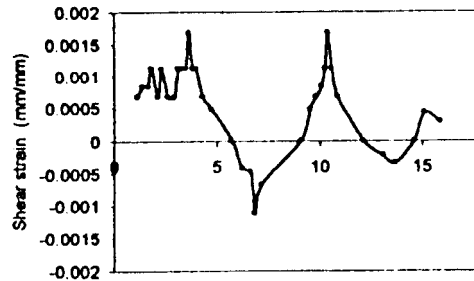


Fig. 6 Shear strains calculated along Section C-C from figure 4a.

6. CONCLUSIONS

This study presented preliminary results on research using moiréinterferometry to characterize strain distributions in finger-jointed lumber. Strain ratios as high as 3.4 were observed near the finger-joint tips for longitudinal strain, corresponding to 33 percent of the ultimate failure load. This strain ratio was observed to increase as load increased. Various elastic properties of the wood adherends on each side of the joint were also determined from the moiré fringe patterns. For the adhesive layer, large shear strains were observed at the gluelines. Because the applied tensile load, the geometric dimensions of the sloped adhesive layer, and the adhesive shear strain are known, the data are available for estimating the equivalent elastic properties of the adhesive layer. This is a topic of ongoing research, along with characterizing the effect of a wide range of material properties on full-field strain behavior of finger joints. These results will be used to validate finite element models of structural finger joints and to conduct a shape optimization study for improving finger-joint strength performance.

7. ACKNOWLEDGMENTS

The author acknowledges Professor Robert E. Rowlands and Ragnar K. Palsson, both of the University of Wisconsin-Madison Mechanical Engineering Department, for use of the moiré interferometry equipment and technical assistance.

8. BIBLIOGRAPHICAL REFERENCES

- [1] Luxford, R.F., Krone, R.H., "End joints of various types in Douglas-fir and white oak compared for strength," Report No. 1622, USDA Forest Service, Forest Products Laboratory, Madison, WI, 1953.
- [2] Blomer, A., "A contribution to the theory and design of glued joints in timber engineering construction, with particular reference to spliced and dovetailed glued timber joints," *Die Bautechnik*, vol 38, no 10, p. 325-350, 1961.
- [3] Madsen, B., Littleford, T.W., "Finger joints for structural usage," *Forest Products Journal*, p. 68-73, Feb. 1962.
- [4] Marian, J.E., "A new procedure for wood finger-jointing and its principles," *Holz als Roh-Werkstoff*, vol 26, no 2, p. 41-45, 1968.
- [5] Oberg, J.C., "The new vs. the old in finger joints," *Wood and Wood Products*, vol 5, p. 35, 1961.
- [6] Page, M.W., "Finger jointing," *The Australian Timber Journal*, vol 25, no 5, p. 82-95, 1959.
- [7] Pavlov, V.P., "Joining wood longitudinally with toothed tenons," *Derevo-pererabatyvaivshchaya i Lesokhimicheskaya Promyshlennost'*, vol 3, no 10, p. 5-8, 1954.
- [8] Rajcan, J., Kozelouh, B., "Designing of glued finger joints," *Technologie*, vol 4, no 3, p. 222-228, 1962.
- [9] Roth, A.A., "Finger joint for jointing boards, battens, planks, and other comparable bodies," Patent No. 3,692,340, 1970.
- [10] Selbo, M.L., "Effect of joint geometry on tensile strength of finger joints," *Forest Products Journal*, p. 390-400, Sept. 1963.
- [11] Richards, D.B., "Improved tips for finger joints," *Forest Products Journal*, p. 250-251, June 1963.

- [12] Strickler, M.D., "Impression finger jointing of lumber," *Forest Product Journal*, vol 17, no 10, p. 23–28, 1967.
- [13] Wadkin Woodworking Machinery and Machine Tools, "The die formed end joint," Green Lane Works, Leicester, LE54PF England, 4 p, 1971.
- [14] Alcher, S., Klöck, W., "Finger joint analysis and optimization by elastic, nonlinear and fracture mechanics finite element computations," *International Timber Engineering Conference*, London, England, 1991.
- [15] Jauslin, C., Pellicane, P.J., Gutkowski, R.M., "Finite-element analysis of wood joints," *Journal of Materials in Civil Engineering*, vol 7, no 1, p. 50–58, 1995.
- [16] Milner, H.R., Yeoh, E., "Finite element analysis of glued timber finger joints," *Journal of Structural Engineering*, vol 117, no 3, p. 755–766, 1991.
- [17] Pellicane, P.J., Gutkowski, R.M., Jauslin, C., "Comparison of optically and mechanically measured deformations in a finger-jointed wood tension specimen," *ASTM, Journal of Testing and Evaluation*, vol 23, no 2, p. 136–140, 1995.
- [18] Zink, A.G., Davidson, R.W., Hanna, R.B. "Strain distributions in adhesive wood joints," *Journal of Adhesion*, vol 58, p. 27–43, 1996.
- [19] Hoadley, R.B., "Strain analysis in wood by means of moiré patterns," *Forest Products Journal*, vol 18, no 5, p. 48–50, 1968.
- [20] Hill, J.L., Sewell, J.H., Azzi, V.D., "Continuous observation of drying strain development using bonded strain sensing material," *Forest Products Research Society Annual Meeting*, Denver, CO, 1977.
- [21] Wilkinson, T.L., Rowlands, R.E., "Analysis of mechanical joints in wood," *Experimental Mechanics*, p. 408–414, November, 1981.
- [22] Post, D., Han, B., Ifju, P., *High sensitivity moiré: Experimental analysis for mechanics and materials*, Springer-Verlag, New York, 1994.

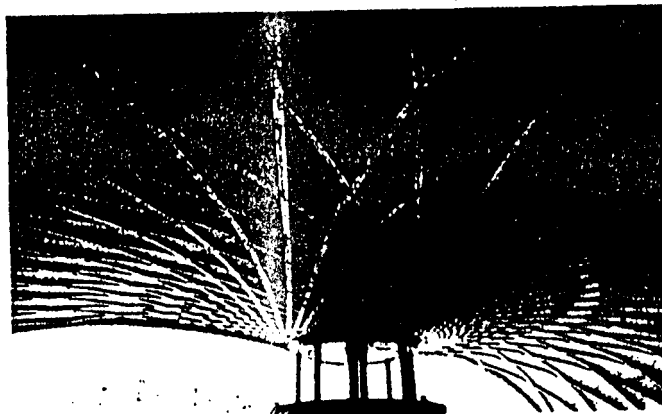


W C T E'98

SWISS FEDERAL
INSTITUTION OF TECHNOLOGY
LAUSANNE-SWITZERLAND

5th WORLD CONFERENCE ON TIMBER ENGINEERING

August 17–20, 1998
Montreux, Switzerland



PROCEEDINGS

Volume 1

Edited by J. Natterer and J.-L. Sandoz

Presses polytechniques et universitaires romandes